Journal of Materials Chemistry A

Designing Solvate Ionogel Electrolytes with Very High Room-Temperature Conductivity and Lithium Transference Number

Journal:	*Journal of Materials Chemistry A*
Manuscript ID	TA-COM-09-2018-008808.R2
Article Type:	Communication
Date Submitted by the Author:	08-Nov-2018
Complete List of Authors:	Hubble, Dion; University of Washington, Molecular Engineering & Sciences Institute Qin, Jiaxu; University of Washington, Molecular Engineering & Sciences Institute Lin, Francis; University of Washington, Chemistry Murphy, Ian; University of Washington, Chemistry Jang, Sei-Hum; University of Washington, Materials Science & Engineering Yang, Jihui; University of Washington, Materials Science and Engineering Jen, Alex K-Y.; University of Washington, Materials Science and Engineering; University of Washington, Chemistry; University of Washington, Molecular Engineering & Sciences Institute; City University of Hong Kong, Materials Science & Engineering

Table of Contents Entry

Designing Solvate Ionogel Electrolytes with Very High Room-Temperature Conductivity and Lithium Transference Number

D. Hubble,[a] J. Qin,[a] F. Lin,[b] I. A. Murphy,[b] S.-H. Jang,[c] J. Yang,[c] and A. K.-Y. Jen[a,b,c,d]

[a] *Molecular Engineering & Sciences Institute, University of Washington, Seattle, WA, 98195, USA*
[b] *Department of Chemistry, University of Washington, Seattle, WA 98195, USA*
[c] *Department of Materials Science and Engineering, University of Washington, Seattle, WA 98195, USA*
[d] *Department of Materials Science and Engineering, City University of Hong Kong, Kowloon, HK*

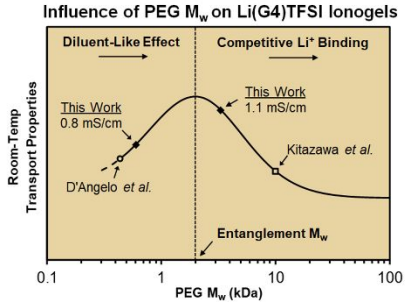

Text: Freestanding gel electrolytes based on Li(G4)TFSI/PEG are demonstrated with enhanced lithium transport and stripping/plating performance due to unique chemical interactions.

Journal of Materials Chemistry A

COMMUNICATION

Designing Solvate Ionogel Electrolytes with Very High Room-Temperature Conductivity and Lithium Transference Number

D. Hubble,[a] J. Qin,[a] F. Lin,[b] I. A. Murphy,[b] S.-H. Jang,[c] J. Yang,[c] and A. K.-Y. Jen[a,b,c,d]

Received 00th January 20xx,
Accepted 00th January 20xx

DOI: 10.1039/x0xx00000x

www.rsc.org/

Free-standing electrolytes based on Li(G4)TFSI and chemically-crosslinked poly(ethylene glycol), as well as functional co-monomers and/or small amounts of volatile diluent, are demonstrated to reach very high room-temperature ionic conductivities (>2×10^{-3} S/cm) and electrochemically-measured lithium transference numbers (>0.5). An unexpected dependence of properties on polymer length/crosslinking is observed and explained in terms of competing Li$^+$ transport processes. These electrolytes enable lithium symmetric cells to cycle >600h at low overpotential and without dendrite growth. Future optimization routes are also discussed.

Introduction

High-capacity energy storage has become increasingly vital in the wireless, networked world of the 21st century. This need has sparked renewed interest in so-called "beyond-lithium-ion" battery designs which often include metallic lithium anodes. However, despite extensive prior research, a safe and practical lithium secondary battery has yet to be realized due to lithium's tendency towards dendritic electroplating morphologies. Dendrites reduce battery capacity and increase internal resistance over time due to electrolyte consumption and formation of "dead" lithium,[1–5] and can even puncture cell separators causing fire and explosion. Recent efforts have yielded numerous materials for lithium dendrite mitigation, broadly classifiable as "host" or "electrolyte" strategies.

Host strategies, which confine lithium to a diverse number of solid structures, can produce excellent electrochemical performance;[6–8] however, they also add "dead weight" and may introduce complications with solid electrolyte interphase (SEI) or electrolyte-soluble intermediates.[9,10] Electrolyte strategies are also diverse, but generally fall into three categories: organic liquid + additive, solid, or concentrated liquid. Traditional carbonate- or ether-based lithium-ion electrolytes, containing ~1M $LiPF_6$ or LiTFSI, possess both high ionic conductivities (κ≈5-20 mS/cm) and lithium transference numbers (t_{Li+}>0.4), enabling large current densities with minimal resistance. Various additives have been proposed to retard dendrite growth/formation in organic formulations without sacrificing their favorable transport properties.[11–14] Alternatively, it has been postulated that a freestanding solid electrolyte of >6GPa elastic modulus can mechanically resist puncture by dendrites.[15] However, the inherently lower ionic conductivity (<1 mS/cm) of solid electrolytes,[16] in addition to contact resistances between discrete particles/surfaces,[17] generally limits their applicability to elevated-temperature systems only. Gel electrolytes, in which a liquid, ion-transporting phase is immobilized by solid components, are often proposed as a middle ground to enhance conductivity while providing limited puncture resistance and avoiding contact issues.[18–22] Gels also provide the opportunity to adjust transport properties using rationally designed interactions between liquid and solid.

Instead of attempting to block dendrites, concentrated electrolytes such as room temperature ionic liquids (RTIL) suppress dendrite formation by dampening space charge formation, which is generally accepted as the fundamental cause of – though not the sole factor in – dendritic growth.[23] Lithium deposits in RTILs trend towards smoother, more uniform morphology as compared to traditional electrolyte solutions,[24–27] although dendrites may still form given enough time or current density.[24] Additional benefits include wide electrochemical windows and non-volatility/flammability, as well as application-specific advantages for certain battery chemistries. However, while Li$^+$-containing RTIL blends can approach the conductivity of organic electrolytes, the transference number of lithium (t_{Li+}) in such blends is very poor,[28,29] limiting high-rate performance.[30,31] Furthermore, the

[a] Molecular Engineering & Sciences Institute, University of Washington, Seattle, WA, 98195, USA
[b] Department of Chemistry, University of Washington, Seattle, WA 98195, USA
[c] Department of Materials Science and Engineering, University of Washington, Seattle, WA 98195, USA
[d] Department of Materials Science & Engineering, City University of Hong Kong, Kowloon, HK

Electronic Supplementary Information (ESI) available: [Materials/equipment, synthetic details, fabrication and characterization]. See DOI: 10.1039/x0xx00000x

lack of existing large-scale RTIL production results in comparatively high prices, limiting practical applicability. Solvate ionic liquids (SILs) have recently emerged as an answer. The 1:1 molar combination of tetraglyme (G4) with lithium bis(trifluoromethanesulfonyl)imide (LiTFSI) forms a strongly-bound chelate complex $[Li(G4)]^+$ that is only weakly associated with its $TFSI^-$ counterion, resulting in a glass-forming ionic liquid that is stable between 0-4.5V vs Li/Li^+, with ionic conductivity >1mS/cm at room temperature.[32–35] Unlike ternary RTIL blends, all cations in Li(G4)TFSI contain lithium, resulting in much higher t_{Li+}. Additionally, G4 and LiTFSI are commercially produced at-scale, making costs more palatable.

In order to combine these advantages with the puncture resistance and molecular design potential of gels, a so-called solvate ionogel (SIG) may be formed by swelling Li(G4)TFSI into a compatible solid host. However, while examples of RTIL ionogels are plentiful, there have been only a handful of recent reports on SIGs.[32,36–38] Their conductivities range 0.1-1 mS/cm at room temperature, similar to other state-of-the-art solid electrolytes but 1-2 orders of magnitude below liquid option. Optimized designs with better conductivity and further improved t_{Li+} could elevate this class of materials into more serious consideration. Nevertheless, the pathway remains unclear, as existing reports seem to disagree with one another. For example, two recent publications[37,38] describe designs based on SIL-miscible poly(ethylene glycol) (PEG), but while D'Angelo *et al.* report that PEG elevates their material's t_{Li+}, Kitazawa *et al.* find the exact opposite. Critically, PEG molecular weights in these materials are vastly different (~450Da vs. 10,000Da). Further complicating things, reported transference numbers for SILs/SIGs are calculated from ion self-diffusion coefficients, which ignores correlated ion motion under applied fields (*e.g.* pairing/clustering).[39,40] Despite these shortcomings, the properties reported for SIGs so far, notwithstanding simple design and limited understanding, suggests a golden opportunity to break the long-standing barrier between liquid and solid electrolytes, provided an appropriate design rationale.

To this end, we report a series of SIGs, each prepared from Li(G4)TFSI immobilized in chemically-crosslinked poly(ethylene gycol) dimethacrylate (PEGDMA). In order to probe the relationship between structural motifs and cell-relevant properties, we iteratively alter our design through variation of PEG length and addition of functionalized co-monomers, as well as slight dilution with an appropriate solvent to produce a "diluted solvate ionogel" (DSIG). Not only do these alterations produce amongst the highest room-temperature conductivities and lithium transference numbers ever reported for ionogel electrolytes – in addition to excellent Li stripping/plating performance – but they also suggest a mechanistic rationale for transport behavior in PEG/Li(G4)TFSI systems which could resolve seeming contradictions in literature. Hence, this report represents a first step towards free-standing electrolytes for lithium secondary cells with truly competitive performance.

Results & Discussion

Five unique compositions of ionogel were fabricated (SIGs 1-5), each containing 80 vol% of liquid electrolyte with 20 vol% polymerizable components (~17 wt% polymer). The formula-specific constituents (**Figure 1a**) were stirred together with a small amount of radical initiator to form transparent, homogeneous solutions, which were then cured at 80°C for 6h in a glass mold (as detailed in the ESI). This process produced thin, freestanding gel films which could be handled and die-cut into circular samples of any desired diameter (**Figure 1b**), which we used to test ionic conductivity (**Figure 1c**), potentiostatic-polarization-based t_{Li+} (**Figure S1**),[41] and compressive elastic modulus (**Figure S2**) of SIGs 1-5 in a climate controlled (23°C) environment. Results are summarized in **Table 1**.

Elastic modulus, important for cell integrity and also linked directly to lithium deposition morphology,[5] ranged 228-401 kPa for our materials, similar to other PEG-based gel electrolytes. While variation between formulas is relatively minor, the differences are simple to correlate with composition. Elongation of polymer chain length from PEGDMA M_n~750 (P_{750}) to PEGDMA M_n~3500 (P_{3500}) produces a decrease in stiffness between SIGs 1 and 2, consistent with larger molecular weight between crosslinks.[42] Replacing half of this P_{3500} with chemically-similar tri(ethylene glycol) methyl ether methacrylate (TEGMA) in SIG 3 does not appear to significantly alter the modulus, while incorporating a small amount of cyclic ether 1,4-dioxane (DSIG 5) produces only a minor decrease. This can be explained by a slight reduction in overall solvent quality for PEG[43,44] for which dioxane is a theta solvent[45] while

Formula	Composition [vol % added]						Properties		
	P_{750}	P_{3500}	TEGMA	PyrTFSIMA	Li(G4)TFSI	Dioxane	E [kPa]	t_{Li+}	κ [mS/cm]
Li(G4)TFSI	0%	0%	0%	0%	100%	0%	n/a	0.13	1.08
SIG 1	20%	0%	0%	0%	80%	0%	369	0.21	0.73
SIG 2	0%	20%	0%	0%	80%	0%	254	0.28	1.05
SIG 3	0%	10%	10%	0%	80%	0%	249	0.24	0.92
SIG 4	0%	10%	0%	10%	80%	0%	401	0.16	1.07
(D)SIG 5	0%	20%	0%	0%	66.6%	13.3%	228	0.57	2.15

Table 1 Composition of five novel SIGs and their measured properties at room temperature (23°C), along with neat SIL for comparison. Reported conductivities are the average of at least three measurements on separate samples.

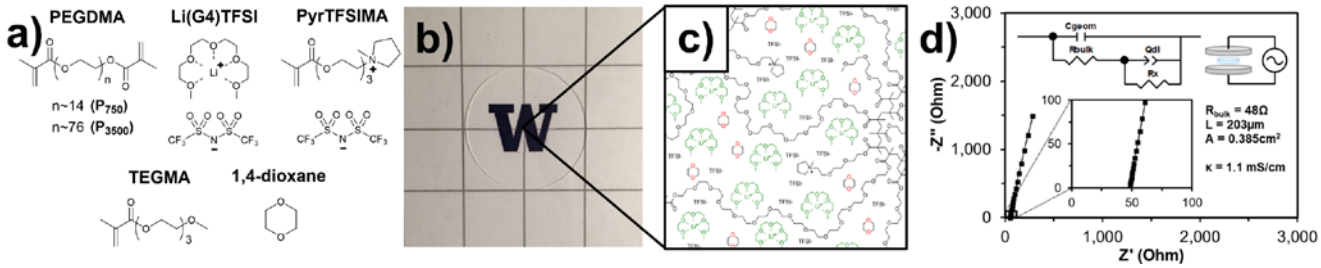

Fig. 1 a) Structures/abbreviations of molecules used to form SIGs. **b)** Photograph of a typical 19mm diameter x 0.25mm thick SIG sample. **c)** Schematic snapshot of SIG molecular structure, showcasing the interplay between solid and liquid components. **d)** Nyquist plot of representative impedance data (10kHz-100Hz) for a SIG 2 sample, used to calculate room-temperature conductivity (Equation S1), with fitted equivalent circuit (upper left).

Li(G4)TFSI is a theta-good solvent.[46] The introduction of ionic-liquid-like pendant group PyrTFSIMA (N-[2-(2-(2-(methacryloyloxy)ethoxy)ethoxy)-ethyl]-N-methyl-pyrrolidium bis(trifluoromethanesulfonyl)imide), as in SIG 4, confers a noticeable increase in modulus, consistent with electrostatic interactions between RTIL and polymer network.[47,48] Interestingly, the trend in resistance to deformation at high stress (SIG 1 < SIG 3 ~ SIG 4 < DSIG 5 ~ SIG 2), inferred by the strain evolved at maximum pressure, is very different than the trend in resistance to deformation at low stress *i.e.* elastic modulus (DSIG 5 ~ SIG 2 ~ SIG 3 < SIG 1 < SIG 4). This is likely a product of increased chain entanglement for gels based on P_{3500} as opposed to P_{750}, the latter being below PEG's entanglement molecular weight of ~2kDa,[49] as well as decreased entanglement in samples with a lower overall number of crosslinking chains (SIGs 3 and 4).[50] In a simplified way, entanglement may be thought of as restricted chain motion caused by adjacent chains crossing one another,[51] which only occurs in sufficiently concentrated polymer solutions above a structure-dependent molecular weight. We were unable to quantitatively measure toughness in our samples, as none of them failed catastrophically up to the maximum pressure achievable in our experiment (325 kPa), but the ability of SIGs to withstand this compressive stress bodes well for their applicability to pouch cells and other non-rigid battery designs.

The lithium transport properties of our SIGs exhibit more significant variation. While "baseline" SIG 1 displayed a room-temperature ionic conductivity of 0.79 mS/cm – slightly higher than, but similar to, SIGs with related designs[37] – increasing PEG molecular weight from P_{750} to P_{3500} produced a nearly 50% increase in conductivity, elevating SIG 2 to near Li(G4)TFSI itself at >1 mS/cm. Critically, this occurs without any change to overall polymer volume fraction. Lithium transference number also increased between samples by 33%, from 0.21 to 0.28. We note that while these t_{Li+} values are higher than most RTIL-based materials, including Li(G4)TFSI itself (measured here as 0.13), all three electrochemically-derived values fall significantly below previous reports of t_{Li+}>0.5 for Li(G4)TFSI, a product of our differing measurement technique. This highlights the importance of obtaining t_{Li+} electrochemically for SIL-based materials, as PGSE-NMR-derived self-diffusion coefficients reveal important structural information but do not reflect transport under applied electric fields for non-ideal electrolytes.[29,40,52,53] Regardless, the properties of SIG 2 are exciting but anomalous, defying the conventional wisdom that gelation of an electrolyte solution reduces its conductivity.

Further variation of the SIG formula provides clues to the transport mechanism. Co-polymerization of monofunctional groups with crosslinkers has previously proven effective at manipulating gel properties,[48,54,55] and here we do so using either neutral (TEGMA) or ionic (PyrTFSIMA) groups of similar structure, while maintaining a constant polymer volume. In the neutral case (SIG 3), this replacement actually slightly worsened both κ (0.92 mS/cm) and t_{Li+} (0.24). We observe that the molar volume ratio of PEG functionality to methacrylate functionality is greatly decreased in TEGMA (3 repeat units per methacrylate) as opposed to P_{3500} (~38 repeat units per methacrylate). Methacrylate functionality has been previously indicated as electrochemically inactive towards Li(G4)TFSI.[37,38,56]

The fact that κ and t_{Li+} decrease concurrently with total volume of PEG suggests a volume-dependent effect of PEG on ion mobility, although we cannot fully decouple this effect from associated, minor changes to the network structure as well. SIG 4, in contrast to its neutral counterpart, displays nearly identical conductivity to SIG 2, but significantly worsened t_{Li+}. This results from additional, mobile anions contributed by ionic-liquid-like PyrTFSIMA, which increases the number of charge carriers but imbalances the ratio away from $[Li(G4)]^+$. This effect can be helpful for dendrite prevention,[57–59] but must be weighed against the subsequent decrease in t_{Li+} which limits current density in practical cells.[60]

In contrast to SIGs 3 and 4, where polymer structure is altered, replacing a small volume of the liquid Li(G4)TFSI with solvent diluent to produce DSIG 5 more than doubled both conductivity (2.15 mS/cm) and t_{Li+} (0.57) compared to SIG 2. To our knowledge, this is the first demonstration of an electrochemically-measured t_{Li+}>0.5 in a SIG-based material, as well the first demonstration of solvent dilution applied to an immobilized SIL and of 1,4-dioxane as a diluent for Li(G4)TFSI in general. The beneficial effect of diluents on SIL properties are well-documented,[34,61,62] and dioxane is an ideal choice for this system: it is a low-molecular-weight solvent that is miscible with all other components, unreactive towards methacrylate radicals, and boils well above the curing temperature of the gel (101°C vs. 80°C), but has too low a dielectric constant to interfere with $[Li(G4)]^+$ structure.[61] The "innocence" of dioxane in this system is further supported by Raman spectroscopy

(**Figure S6**). The exact mechanism by which solvent dilution affects electrochemical, rather than diffusion-based, t_{Li+} in SILs has yet to be clarified. However, we are not the first to report increased t_{Li+} upon diluting a SIL. This effect seems highly volume-dependent: at least one prior study has indicated a large t_{Li+} increase for a diluted SIL when solvent volume fraction becomes ~23-33% of the total,[27] similar to the combined volume of P_{3500}/dioxane in DSIG 5. Altogether, this hints at a "diluent-like" effect of PEG.

To further explore the idea of PEG-as-diluent, we prepared non-crosslinked versions of SIGs 1 and 2, referred to as LIQ 1 and LIQ 2, which differed only in absence of a crosslinking initiator. However, counterintuitively, we found that room-temperature conductivity *decreased* in the liquid state, and that the trend with molecular weight is reversed (LIQ 1: 0.72 mS/cm, LIQ 2: 0.57 mS/cm), indicating that transport in PEG/Li(G4)TFSI mixtures depends significantly on whether the polymer is crosslinked or not.‡ Notably, PEO/LiTFSI solid electrolytes show the same trend in conductivity vs. molecular weight when M_w<4kDa *i.e.* from below to just above the entanglement limit. This has been ascribed to vanishing mobility of polymer/Li^+ complexes (as opposed to interchain Li^+ transport *via* segmental motion) above the entanglement limit.[63] In point of fact, it has been previously shown that PEG can compete with G4 for Li^+ binding in Li(G4)TFSI *i.e.* it is a "non-innocent" diluent,[38,56] which induces formation of polymer/Li^+ complexes.

With all of the above information we may begin to rationalize the transport behavior of PEG/Li(G4)TFSI mixtures, including SIGs. We posit that competitive binding of Li^+ and "diluent-like" mobility enhancement are simultaneous-but-competing effects which depress or enhance Li^+ transport, respectively (**Figure 2**). Because the stability of $[Li(polyether)]^+$ complexes depends strongly on change in entropy upon binding *i.e.* the chelate effect,[64,65] the ability of PEG to effectively compete with G4 for Li^+ must be dependent on polymer conformational freedom. Chemical crosslinking results in a significant loss of freedom, especially for chain segments near the crosslinking sites,[44,66] which should therefore shift the competitive equilibrium more strongly towards G4. Competitive Li^+ binding by PEG in SILs is indirectly detectable through thermogravimetry,[38] as the liberated G4 molecules are slightly volatile at 120°C. We do indeed observe greater weight loss at 120°C for the liquid vs. crosslinked samples (**Figure S3**), suggesting that the stability of the $[Li(G4)]^+$ complex is affected by PEG crosslinking status. Interestingly, while one might expect the shorter, un-entangled P_{750} to displace G4 more readily than P_{3500} in the solution state, the difference in weight loss with crosslinking is actually smaller for the smaller chain, which may point towards some fundamental difference in PEG/Li(G4)TFSI interaction below the entanglement limit.

PEG chain segments that do not compete for Li^+ may instead exert a diluent-like effect. Solvent dilution of RTILs tends to greatly reduce their viscosity and thus improve ion mobility, albeit with a concurrent, dielectric-dependent reduction of ionicity as well.[67–69] In lithium SILs, where cation molecular structure may also fluctuate,[70] diluents can additionally affect the structure and balance of Li^+-G4 complexes.[61] Regardless,

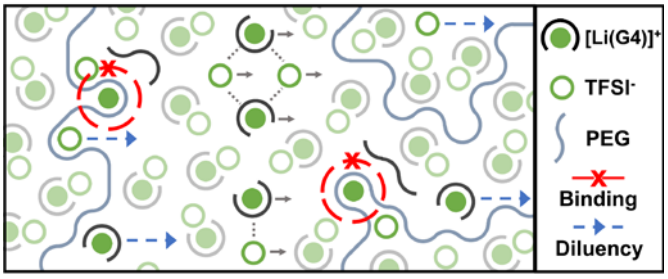

Fig. 2 Schematic diagram of PEG/Li(G4)TFSI interactions under an applied field, conceptually depicting competitive binding of Li^+ and diluent-like mobility enhancement by PEG.

PEG fits the criteria for an effective SIL diluent, possessing a moderate dielectric constant of ~4 and a donor number similar to glymes. In fact, studies which report lowered D_{Li+} in PEG/Li(G4)TFSI systems also report improved bulk conductivity relative to other polymer choices.[38,56] These effects could only occur simultaneously if the depressed mobility of bound Li^+ is outweighed, on average, by enhanced mobility for the remaining ions *i.e.* a diluent-like effect. Furthermore, our own results lead us to postulate that this enhancement is influenced by 1) the volume fraction of PEG relative to total SIL-swelled polymer, and, for crosslinked systems, 2) whether the molecular weight between crosslinks is above or below the entanglement molecular weight of PEG (~2kDa).

Plasticization of the polymer network, often invoked to explain transport in solid polymer electrolytes,[71] does not seem to be a major factor, as differential scanning calorimetry data indicates an increase, rather than decrease, of T_g for samples with P_{3500} (**Figure S4**), perhaps a result of more $[Li(polyether)]^+$ complex formation. Instead, the observed dependence on polymer molecular weight is likely caused by specific chemical interactions. It is possible that, rather than being directly related to entanglement itself, enhanced mobility at higher M_w is related the radius of gyration of the polymer in comparison to the bulky sizes of $[Li(G4)]^+$, $TFSI^-$, and their aggregates. Further study is needed to clarify the origin of this effect.

The dual action of PEG (binding vs. diluency) on Li(G4)TFSI also accounts for behavior in previously-reported SIG materials. In our SIG 1, as well the SIGs reported by D'Angelo *et al.*, competitive Li^+ binding by PEG is rendered unfavorable due to low molecular weight and/or chemical crosslinking; hence, the volume-dependent diluent-like effect dominates, and both κ and t_{Li+} are observed to increase compared to similar materials lacking PEG. However, the improvement is minor, again due to low molecular weight between crosslinks. On the other hand, the PEG chain in the block copolymer reported by Kitazawa *et al.* is much longer (M_w>10kDa) and also processed at higher temperature, creating opportunities for coiled PEG segments to bind Li^+ and liberate G4. The resulting SIG displays reduced t_{Li+} compared to a methacrylate analog, although κ is still observed to increase overall due to the diluent-like effect.

Our P_{3500}-based SIGs apparently occupy a "sweet spot" between these cases, where molecular weight between crosslinks is large enough to maximize the diluent effect, but not so large that competitive binding of Li^+ overshadows it. This

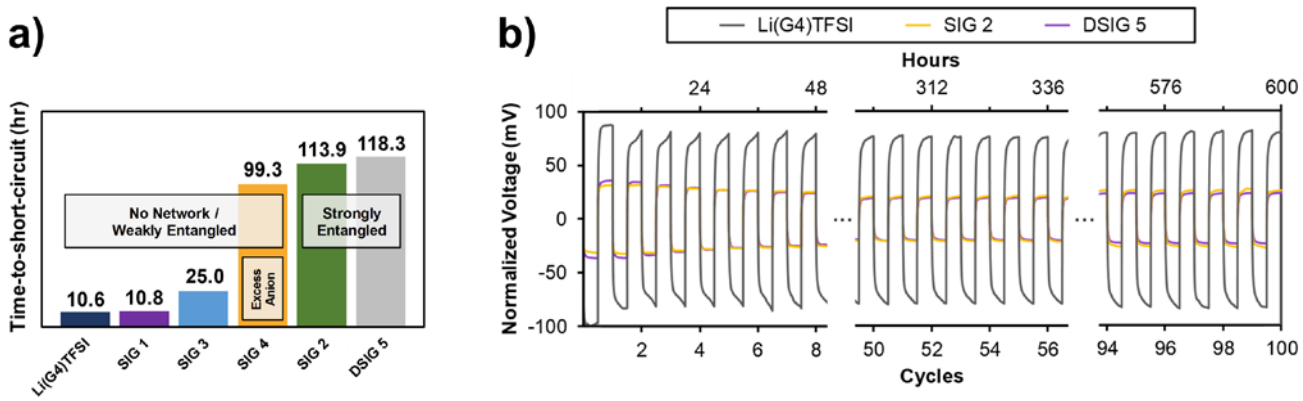

Fig. 3 a) Time-to-short-circuit (0.1 mA/cm^2) for Li|Li symmetric cells with SIG separators vs. Li(G4)TFSI/glass fiber. T_{sc} correlates with volume of (entangled) P_{3500}. Excess mobile anion, as in SIG 4, also has a noticeable effect. **b)** Symmetric cell cycling data for best-performing SIGs, which demonstrate consistent and lower overpotential vs. Li(G4)TFSI/glass fiber. No short circuits were observed through 100 cycles (600 hours) at 0.1 mA/cm^2. Voltage data is normalized to Li(G4)TFSI based on sample/separator thickness to account for batch-to-batch variation and allow a head-to-head comparison.

mechanistic view also suggests that further improvement might be achieved through rational design of the polymer matrix and/or liquid composition to minimize/eliminate competitive binding while maximizing diluent-like properties. We plan to explore this concept in future publications.

In order to confirm that favorable SIG properties translate into good performance with lithium metal, we constructed Li|Li symmetric cells containing SIG separators and performed galvanostatic (0.1 mA/cm^2) polarization experiments at room temperature until lasting short circuits were observed (**Figure S5**). Time-to-short-circuit (T_{sc}) values are summarized in comparison to neat Li(G4)TFSI contained in a large-pore glass fiber separator (**Figure 3a**). While no major advantage over the SIL is observed for SIG 1, SIGs 2-5 show excellent dendrite resistance. Best-performers SIG 2 and DSIG 5, which have the largest concentration of P_{3500}, could resist short-circuit for longer than 100h of continuous current application – competitive with other high-performing gel electrolytes.[72] Using our improved structural insight to analyze these results, it is clear that short-circuit resistance is related to chain entanglement, which should act to dissipate the force of a protruding dendrite more evenly throughout the network. Elastic modulus does not directly reflect this structural detail. High-stress behavior, however, seems to correlate better (*vide supra*), and we suggest that more future efforts be dedicated to studying and correlating non-elastic mechanical properties with dendrite resistance. We also note that SIG 4 performs much better than SIG 3 despite similar network structures, confirming that anion concentration and other chemical details also play a role.

Cyclic stripping/plating in symmetric cells, as opposed to static polarization, more accurately mimics real device conditions. Hence the best-performing SIG 2 and DSIG 5 were compared to Li(G4)TFSI/glass fiber over 100 6h cycles at 0.1 mA/cm^2 (**Figure 3b**). All cells exhibited an initial SEI formation period with slightly higher overpotential and irregular voltage profile shape, followed by minimum overpotential around the 50 cycle (30h) mark. Continued cycling out to 600 hours results in a very slight increase for all cells, most likely due to gradual SEI buildup, however, no signs of short-circuit were observed, and the shapes of the stabilized profiles was smooth and monotonically increasing, suggesting non-dendritic morphology.[73] Furthermore, both SIGs required significantly less overpotential for stripping/plating than neat Li(G4)TFSI, possibly due to porosity/tortuosity effects in the glass fiber separator.[74] However, comparing SIG 2 with DSIG 5, it is clear that overpotential does not correlate linearly with transport properties. Interfacial resistance likely plays a limiting role in this system, which might be selectively improved through compositional engineering.

Conclusions

In summary, we have fabricated a series of free-standing solvate ionogel (SIGs) electrolytes based on low-cost Li(G4)TFSI immobilized in a chemically-crosslinked poly(ethylene glycol) dimethacrylate (PEGDMA) network. Through careful design of both polymer structure and liquid composition, we have demonstrated the potential to control properties such as conductivity (κ) and lithium transference number (t_{Li+}) to exceed 2×10^{-3} S/cm and 0.5, respectively. Additionally, we have uncovered a significant dependence of lithium transport on PEG chain length and crosslinking status in SIGs, which may be due to an interplay between competitive Li^+ binding and "diluent-like" mobility enhancement that changes for PEG above the entanglement limit (~2kDa). These outstanding properties make SIGs well-suited for lithium metal batteries, with best-performing formulas able to strip/plate lithium for >600h (100 cycles) without short-circuiting. Our results also suggest future areas for SIG optimization, such as reduction of competitive Li^+ binding, reduction of lithium interfacial resistance, and improved toughness. The combination of simple fabrication, excellent Li^+ transport, and metallic lithium compatibility makes SIGs attractive for "beyond Li-ion" battery designs.

Conflicts of interest

There are no conflicts to declare.

Acknowledgements

This material is based upon work supported by the Department of Energy, Office of Energy Efficiency and Renewable Energy (EERE), under Award Number DE-EE0007791. D. H. acknowledges government support under and awarded by the Department of Defense, Air Force Office of Scientific Research, National Defense Science and Engineering Graduate (NDSEG) Fellowship, 32 CFR 168a. D. H. additionally thanks Ryan Toivola for assistance with mechanical testing.

Notes and references

‡ t_{Li+} could not be accurately measured for LIQs 1 and 2 due to extremely high interfacial resistance in symmetric cells containing these samples.

1 D. Lv, Y. Shao, T. Lozano, W. D. Bennett, G. L. Graff, B. Polzin, J. Zhang, M. H. Engelhard, N. T. Saenz, W. A. Henderson, P. Bhattacharya, J. Liu and J. Xiao, *Adv. Energy Mater.*, 2015, **5**, 1–7.
2 D. Lin, Y. Liu and Y. Cui, *Nat. Nanotechnol.*, 2017, **12**, 194–206.
3 X. B. Cheng, R. Zhang, C. Z. Zhao, F. Wei, J. G. Zhang and Q. Zhang, *Adv. Sci.*, 2015, **3**, 1–20.
4 K. Xu, *Chem. Rev.*, 2014, 114, 11503–11618.
5 M. D. Tikekar, S. Choudhury, Z. Tu and L. A. Archer, *Nat. Energy*, 2016, **1**, 1–7.
6 L. Liu, Y. X. Yin, J. Y. Li, S. H. Wang, Y. G. Guo and L. J. Wan, *Adv. Mater.*, 2018, **30**, 1–8.
7 D. Lin, J. Zhao, J. Sun, H. Yao, Y. Liu, K. Yan and Y. Cui, *Proc. Natl. Acad. Sci.*, 2017, **114**, 4613–4618.
8 Z. Liang, D. Lin, J. Zhao, Z. Lu, Y. Liu, C. Liu, Y. Lu, H. Wang, K. Yan, X. Tao and Y. Cui, *Proc. Natl. Acad. Sci.*, 2016, **113**, 2862–2867.
9 Q. Pang, X. Liang, C. Y. Kwok and L. F. Nazar, *Nat. Energy*, 2016, **1**, 1–11.
10 W.-J. Kwak, J.-B. Park, H.-G. Jung and Y.-K. Sun, *ACS Energy Lett.*, 2017, **2**, 2756–2760.
11 F. Ding, W. Xu, G. L. Graff, J. Zhang, M. L. Sushko, X. Chen, Y. Shao, M. H. Engelhard, Z. Nie, J. Xiao, X. Liu, P. V. Sushko, J. Liu and J. G. Zhang, *J. Am. Chem. Soc.*, 2013, **135**, 4450–4456.
12 Y. Lu, Z. Tu and L. A. Archer, *Nat. Mater.*, 2014, **13**, 961–969.
13 J. Guo, Z. Wen, M. Wu, J. Jin and Y. Liu, *Electrochem. commun.*, 2015, **51**, 59–63.
14 R. Miao, J. Yang, X. Feng, H. Jia, J. Wang and Y. Nuli, *J. Power Sources*, 2014, **271**, 291–297.
15 C. Monroe and J. Newman, *J. Electrochem. Soc.*, 2005, **152**, A396.
16 F. Zheng, M. Kotobuki, S. Song, M. O. Lai and L. Lu, *J. Power Sources*, 2018, **389**, 198–213.
17 A. C. Luntz, J. Voss and K. Reuter, *J. Phys. Chem. Lett.*, 2015, **6**, 4599–4604.
18 K. M. Abraham, Z. Jiang and B. Carroll, *Chem. Mater.*, 1997, **9**, 1978–1988.
19 G. B. Appetecchi, G. T. Kim, M. Montanino, M. Carewska, R. Marcilla, D. Mecerreyes and I. De Meatza, *J. Power Sources*, 2010, **195**, 3668–3675.
20 R. He and T. Kyu, *Macromolecules*, 2016, **49**, 5637–5648.
21 R. Khurana, J. L. Schaefer, L. A. Archer and G. W. Coates, *J. Am. Chem. Soc.*, 2014, **136**, 7395–7402.
22 P. Pal and A. Ghosh, *Electrochim. Acta*, 2018, **278**, 137–148.
23 J. N. Chazalviel, *Phys. Rev. A*, 1990, **42**, 7355–7367.
24 P. C. Howlett, D. R. MacFarlane and A. F. Hollenkamp, *Electrochem. Solid-State Lett.*, 2004, **7**, A97.
25 L. Suo, Y.-S. Hu, H. Li, M. Armand and L. Chen, *Nat. Commun.*, 2013, **4**, 1481.
26 L. Grande, J. Von Zamory, S. L. Koch, J. Kalhoff, E. Paillard and S. Passerini, *ACS Appl. Mater. Interfaces*, 2015, **7**, 5950–5958.
27 H. Wang, M. Matsui, H. Kuwata, H. Sonoki, Y. Matsuda, X. Shang, Y. Takeda, O. Yamamoto and N. Imanishi, *Nat. Commun.*, 2017, **8**, 15106.
28 T. Frömling, M. Kunze, M. Schönhoff, J. Sundermeyer and B. Roling, *J. Phys. Chem. B*, 2008, **112**, 12985–12990.
29 F. Wohde, M. Balabajew and B. Roling, *J. Electrochem. Soc.*, 2016, **163**, A714–A721.
30 H. Yoon, P. C. Howlett, A. S. Best, M. Forsyth and D. R. MacFarlane, *J. Electrochem. Soc.*, 2013, **160**, A1629–A1637.
31 K. Yoshida, M. Tsuchiya, N. Tachikawa, K. Dokko and M. Watanabe, *J. Electrochem. Soc.*, 2012, **159**, A1005–A1012.
32 T. M. Pappenfus, W. A. Henderson, B. B. Owens, K. R. Mann and W. H. Smyrl, *J. Electrochem. Soc.*, 2004, **151**, A209.
33 T. Tamura, K. Yoshida, T. Hachida, M. Tsuchiya, M. Nakamura, Y. Kazue, N. Tachikawa, K. Dokko and M. Watanabe, *Chem. Lett.*, 2010, **39**, 753–755.
34 K. Yoshida, M. Tsuchiya, N. Tachikawa, K. Dokko and M. Watanabe, *J. Phys. Chem. C*, 2011, **115**, 18384–18394.
35 K. Ueno, K. Yoshida, M. Tsuchiya, N. Tachikawa, K. Dokko and M. Watanabe, *J. Phys. Chem. B*, 2012, **116**, 11323–11331.
36 Y. Kitazawa, K. Iwata, S. Imaizumi, H. Ahn, S. Y. Kim, K. Ueno, M. J. Park and M. Watanabe, *Macromolecules*, 2014, **47**, 6009–6016.
37 A. J. D'Angelo and M. J. Panzer, *J. Phys. Chem. B*, 2017, **121**, 890–895.
38 Y. Kitazawa, K. Iwata, R. Kido, S. Imaizumi, S. Tsuzuki, W. Shinoda, K. Ueno, T. Mandai, H. Kokubo, K. Dokko and M. Watanabe, *Chem. Mater.*, 2018, **30**, 252–261.
39 G. Feng, M. Chen, S. Bi, Z. A. H. Goodwin, E. B. Postnikov, M. Urbakh and A. A. Kornyshev, .
40 D. R. MacFarlane, M. Forsyth, E. I. Izgorodina, A. P. Abbott, G. Annat and K. Fraser, *Phys. Chem. Chem. Phys.*, 2009, **11**, 4962–4967.
41 J. Evans, C. A. Vincent and P. G. Bruce, *Polymer*, 1987, **28**, 2324–2328.
42 P.-G. de Gennes, *Scaling Concepts in Polymer Physics*, Cornell University Press, Ithaca, NY, 1979.
43 M. Zrinyi and F. Horkay, *Polymer*, 1987, **28**, 1139–1143.
44 Y. Huang, I. Szleifer and N. A. Peppas, *Macromolecules*, 2002, **35**, 1373–1380.
45 J. E. Mark, Ed., *Polymer Data Handbook*, Oxford University Press, New York, NY, 1999.
46 Z. Chen, P. A. Fitzgerald, G. G. Warr and R. Atkin, *Phys. Chem. Chem. Phys.*, 2015, **17**, 14872–14878.
47 M. Rubinstein, R. H. Colby, A. V. Dobrynin and J. F. Joanny, *Macromolecules*, 1996, **29**, 398–406.
48 Y. Ding, J. Zhang, L. Chang, X. Zhang, H. Liu and L. Jiang, *Adv. Mater.*, 2017, **29**, 1704253.
49 Poly(ethylene glycol), http://polymerdatabase.com/polymers/polyethyleneglycol.html, (accessed 28 July 2018).
50 X. Zhao, *Proc. Natl. Acad. Sci.*, 2017, **114**, 8138–8140.
51 A. E. Likhtman and M. Ponmurugan, *Macromolecules*, 2014, **47**, 1470–1481.
52 K. M. Diederichsen, E. J. McShane and B. D. McCloskey, *ACS Energy Lett.*, 2017, acsenergylett.7b00792.
53 M. Chintapalli, K. Timachova, K. R. Olson, S. J. Mecham, D. Devaux, J. M. Desimone and N. P. Balsara, *Macromolecules*, 2016, **49**, 3508–3515.
54 A. S. Shaplov, D. O. Ponkratov, P. S. Vlasov, E. I. Lozinskaya, L. V. Gumileva, C. Surcin, M. Morcrette, M. Armand, P.-H. Aubert, F. Vidal and Y. S. Vygodskii, *J. Mater. Chem. A*, 2015, **3**, 2188–2198.
55 A. S. Shaplov, D. O. Ponkratov, P.-H. Aubert, E. I. Lozinskaya, C. Plesse, A. Maziz, P. S. Vlasov, F. Vidal and Y. S. Vygodskii, *Polymer*, 2014, **55**, 3385–3396.
56 R. Kido, K. Ueno, K. Iwata, Y. Kitazawa, S. Imaizumi, T. Mandai,

K. Dokko and M. Watanabe, *Electrochim. Acta*, 2015, **175**, 5–12.
57 Y. Lu, S. K. Das, S. S. Moganty and L. A. Archer, *Adv. Mater.*, 2012, **24**, 4430–4435.
58 Y. Lu, K. Korf, Y. Kambe, Z. Tu and L. A. Archer, *Angew. Chemie - Int. Ed.*, 2014, **53**, 488–492.
59 S. Choudhury, R. Mangal, A. Agrawal and L. A. Archer, *Nat. Commun.*, 2015, **6**, 1–9.
60 J. Newman and K. E. Thomas-Alyea, *Electrochemical Systems*, John Wiley & Sons Inc., Hoboken, NJ, 3rd edn., 2004.
61 K. Ueno, J. Murai, K. Ikeda, S. Tsuzuki, M. Tsuchiya, R. Tatara, T. Mandai, Y. Umebayashi, K. Dokko and M. Watanabe, *J. Phys. Chem. C*, 2016, **120**, 15792–15802.
62 K. Dokko, N. Tachikawa, K. Yamauchi, M. Tsuchiya, A. Yamazaki, E. Takashima, J.-W. Park, K. Ueno, S. Seki, N. Serizawa and M. Watanabe, *J. Electrochem. Soc.*, 2013, **160**, A1304–A1310.
63 A. A. Teran, M. H. Tang, S. A. Mullin and N. P. Balsara, *Solid State Ionics*, 2011, **203**, 18–21.
64 R. D. Hancock, *J. Chem. Educ.*, 1992, **69**, 615.
65 C. Zhang, K. Ueno, A. Yamazaki, K. Yoshida, H. Moon, T. Mandai, Y. Umebayashi, K. Dokko and M. Watanabe, *J. Phys. Chem. B*, 2014, **118**, 5144–5153.
66 P. Flodin and P. Lagerkvist, *J. Chromatogr. A*, 1981, **215**, 7–12.
67 H. Tokuda, S.-J. Baek and M. Watanabe, *Electrochemistry*, 2005, **73**, 620–622.
68 W. Li, Z. Zhang, B. Han, S. Hu, Y. Xie and G. Yang, *J. Phys. Chem. B*, 2007, **111**, 6452–6456.
69 P. M. Bayley, G. H. Lane, N. M. Rocher, B. R. Clare, A. S. Best, D. R. MacFarlane and M. Forsyth, *Phys. Chem. Chem. Phys.*, 2009, **11**, 7202.
70 W. Shinoda, Y. Hatanaka, M. Hirakawa, S. Okazaki, S. Tsuzuki, K. Ueno and M. Watanabe, *J. Chem. Phys.*, 2018, **148**, 193809.
71 D. Bamford, A. Reiche, G. Dlubek, F. Alloin, J. Y. Sanchez and M. A. Alam, *J. Chem. Phys.*, 2003, **118**, 9420–9432.
72 X. B. Cheng, R. Zhang, C. Z. Zhao and Q. Zhang, *Chem. Rev.*, 2017, **117**, 10403–10473.
73 K. N. Wood, E. Kazyak, A. F. Chadwick, K. H. Chen, J. G. Zhang, K. Thornton and N. P. Dasgupta, *ACS Cent. Sci.*, 2016, **2**, 790–801.
74 B. Tjaden, S. J. Cooper, D. J. Brett, D. Kramer and P. R. Shearing, *Curr. Opin. Chem. Eng.*, 2016, **12**, 44–51.

